DEUTSCHES ELEKTRONEN-SYNCHROTRON DESY

DESY SR-77/21
December 1977

Soft X-Ray Microscopy and Lithography with Synchrotron Radiation

by

Wolfgang Gudat

NOTKESTRASSE 85 · 2 HAMBURG 52

To be sure that your preprints are promptly included in the
HIGH ENERGY PHYSICS INDEX ,
send them to the following address (if possible by air mail) :

DESY
Bibliothek
Notkestrasse 85
2 Hamburg 52
Germany

SOFT X-RAY MICROSCOPY AND LITHOGRAPHY WITH SYNCHROTRON RADIATION

Wolfgang Gudat

Deutsches Elektronen-Synchrotron DESY, D-2000 Hamburg 52

Considerable progress in the technique microscopy with soft x-ray radiation has been achieved in particular through the application of synchrotron radiation. Various methods which are currently being studied theoretically or already being used practically will be described briefly. Attention is focussed on the method of contact microscopy. Various biological specimens have been investigated by this method with a resolution as good as 100 Å. X-ray lithography which in the technical procedure is very similar to contact microscopy gives promise for the fabrication of high quality submicron structures in electronic device production. Important factors limiting the resolution and determining the performance of contact microscopy and x-ray lithography will be discussed.

Introduction

More than sixty years ago Goby[1] used x-rays to expose a photographic emulsion with a specimen placed in front of it. After development he viewed the film in an optical microscope. This was the beginning of x-ray microscopy. In the following years Goby's technique of contact microradiography or contact x-ray microscopy has been improved by several workers[2,3]. In addition, various alternative methods have been explored to obtain magnified images directly with x-rays by using e.g. projection techniques and grazing incidence mirror optics.[2,3] But until recently[4] the resolution obtained with all methods has not been better than that of a good optical microscope, in which the resolution is limited by diffraction effects. Nevertheless, x-ray microscopy has been used considerably in biological and medical research and to a certain extent in metallography.[2,3] The main reasons were large penetration depth of x-rays and image contrast, in comparison to optical microscopy, which enabled the study of internal structures and the determination of elemental composition of objects.

Obviously, the shortcomings of the early microscopy studies were due to poor resolution and sensitivity of the x-ray detectors, intensity and collimation of x-ray sources and the use of optical microscopes for inspection. In the last years considerable progress in microscopy techniques with soft x-ray radiation has been achieved in particular through the application of high brightness synchrotron radiation, high resolution photosensitive resist materials and scanning electron microscopes. In this paper various methods[4-12] which are currently being studied theoretically or already being used practically will be decribed briefly. Attention is focussed on the method of contact microscopy and its possibilities and limitations will be discussed. In a third section we discuss some aspects of x-ray lithography which in the general technical procedure is very similar to contact microscopy, but which was established as an important step in microelectronic device fabrication.[13-15]

Microscopy with soft x-rays

The attenuation of soft x-rays with wavelength of about 5 Å to 100 Å in matter is almost completely due to photoabsorption and is thus described by Lambert-Beer's law, namely,

$$I = I_o \exp(-\alpha d) = I_o \exp(-\alpha/\rho \cdot \rho d),$$

where I_o is the intensity of the unattenuated beam, while I is the intensity transmitted through matter of density ρ, thickness d and linear absorption coefficient α. Figure 1 shows the linear absorption coefficient α of some highly absorbing and some weakly absorbing materials[16,17] as a function of wavelength. For organic materials the inverse of α, the penetration depth of the radiation, is typically longer than micrometer, whereas in metals with high atomic number the penetration depth is typically smaller than one tenth of micrometer. Since the contrast in soft x-ray microscopy is determined by the absorbed intensity, the preferred wavelength range for high contrast of a given specimen thickness d is clearly in the range $\lambda > 10$ Å. Clearly, for highest resolution work with very thin specimens the longer wavelength range has also to be considered. Its tunability, high intensity and extreme collimation makes synchrotron radiation to a favourable light source in this wavelength range. The peak power of a storage ring with an electron energy of about 350 MeV and standard magnetic field is emitted at about 10 Å and falls off smoothly to longer wavelengths.

Various methods for microscopy with synchrotron radiation have been introduced since 1972. They can be subdivided into two classes; namely into a class which allows "real-time microscopy" at a moderate resolution (but still better than with light microscopy) and a class, which gives potentially the highest resolution in a non-real-time mode. To the former belong the techniques of scanning microscopy,[5,6] the application of mirror optics[7] and of Fresnel zone plates.[8,9] To the latter belong x-ray holography[10,11] and contact microscopy.[4,12]

Figure 2 depicts the technique of scanning microscopy according to Horowitz and Howell . Synchrotron radiation with wavelengths 5 Å to 25 Å is focussed onto a "2 µm pinhole" in a gold absorber. The hole determines a radiation beam which passes through the specimen which is mounted on a x,y-transducer sample holder combination. Gasfilled proportional counters surrounding the beam axis detect the characteristic fluorescent soft x-rays emitted by the specimen. Thus the sample is investigated one point at a time, while being moved in a x-y raster pattern perpendicular to the beam axis. The resolution obtained with metallic grids as samples corresponds to the diameter of the pinhole; i.e. 2 µm. Hole sizes with submicron diameters seem feasible, although they have to be made in material sufficiently thick to attenuate incident x-rays by many orders of magnitude. As a consequence the angular acceptance of the synchrotron light becomes very small, which implies a strong decrease in signal to noise ratio of the detection system. To avoid this problems Spiller[6] suggests to use high quality mirror optics to obtain directly a focal spot of size about 500 Å. Similarly, Schmahl and cowokers[9] want to use Fresnel zone plates as focussing elements in connection with the scanning mechanism.

There is one important advantage with scanning microscopy techniques in contrast to the other methods and that is in connection with radiation damage which is the most severe problem for all high resolution microscopy of living objects. The investigation of living specimens, e.g. embedded in a wet atmosphere between highly transparent films, is certainly one of the major goals for microscopists. For a minimum radiation damage of a biological specimen the x-ray detector behind it should have a quantum efficiency as high as possible, ideally 100 %. There is a general condition which states that any detector requires a certain energy density per resolution element for its activation. This implies that a detector for scanning microscopy, where spatial resolution is not required, most likely has a much higher sensitivity than a detector being used for microscopy techniques

where high spatial resolution is a necessity. In this context it is interesting to note that recent model calculations[18] of the radiation dosage levels to biological specimens in their natural state have shown that these levels are lower in a suboptical regime when specimens are exposed to soft x-rays than to high energetic electrons in an electron microscope.

Niemann, Rudolph and Schmahl[9] have built the first imaging microscope for soft x-ray synchrotron radiation using zone plates as imaging optical elements. In their system a holographically made zone plate (diameter D=5 mm and 2600 zones) generates at a wavelength of 46 Å a reduced image of the radiation source in the object plane. A magnified image (15 x) of the object is directly obtained via a second microzone plate and recorded on high resolution photographic material. With a resolution of about 0.4-0.5 µm pictures of algae, cotton fibres[6] and 3T3 mouse cells in their living state [9]have been obtained. With improved zone plates operating in the 3rd diffraction order, one hopes to achieve a resolution in the order of 500 Å. Haelbich and Kunz[7] studied an imaging microscope for the wavelength range of about 50 - 100 Å which is based on a concentric mirror system (so called Schwarzschild objective) working at near normal incidence in order to avoid the image distortions inherent in grazing incidence optics.[2,19] However, progress in multilayer film deposition[20,21] is required in order to achieve the necessary high reflectivity of the optical components.

In holography both, the amplitude and the phase of a wave pattern of an object are recorded on a photographic plate by means of interference of coherent waves. A three dimensional information on the original object can be reconstructed from the hologram i.e., the developed photo plate, by a simple projection technique with coherent light. If the light sources for recording and for reconstruction have different wavelength a direct magnification is obtained in proportion to

the ratio of the wavelengths. In first demonstration experiments with monochromatized synchrotron radiation (λ=60 Å) Aoki and Kikuta[10] succeeded in taking a picture of a slitsystem with a direct magnification of 158. Using Al K_α radiation x-ray holograms of chemical fibers with dimensions of 2 µm have been recorded.[22] To date the advantages of x-ray holography, namely, no resolution limitation due to diffraction effects and three dimensional pictures of an object at at time, have not been exploited.

Contact Microscopy

In contrast to most of the microscopy techniques described above for contact microscopy no optical component is required between the light source and the specimen and the detector, respectively. Figure 3 schematically shows the arrangement for contact microscopy. A highly polished silicon substrate is coated with a thin film of organic polymer. This resist film acts as a high resolution x-ray sensitive detector, because the polymer is modified by absorbed radiation in such a way that in a subsequent development process exposed regions are dissolved much more strongly than unexposed regions. Specimens are placed on top of the resist and are exposed to soft x-rays. A replica in relief of the specimen's optical density is therefore obtained at a 1:1 magnification via the development procedure (see part II of Fig. 3). The magnification of the replica is most easily obtained with a scanning electron microscope (SEM), thereby exploiting the large depth of focus of the SEM. Since polymers are non-conductors one has to metallize the resist pattern in order to avoid charging during the SEM work.

We have investigated various biological specimens[4,12,15,23] by means of contact microscopy using synchrotron radiation of the DESY-synchrotron. Our experiments were performed in evacuated sample chambers which were located at two different beamlines at a distance of about 40 m from the source point. In a "direct beamline" the samples could be exposed to the full spectrum of synchrotron radiation

of DESY running at energies 3 to 7 GeV. In a second beam line we used a 4° grazing incidence mirror with a gold coating as a short wavelength cut-off element (about 20 - 25 Å depending on surface condition) in order to avoid exposure with such wavelengths which produce only very weak contrast. Figures 4a-4c show soft x-ray replicas of diatoms in PMMA resist (polymethyl methacrylate-used here) obtained at the 4° beam with typical exposure times of about 10 minutes. These pictures[4] already demonstrate that structural details of 1000 Å width or less are reproduced. It is of course desirable to extend microscopy studies towards an examination of biological specimens with soft x-ray radiation of different, well defined wavelength. As a first step towards that direction we studied critically point dried heart of chick embryo cells[23] with synchrotron radiation with an effective wavelength range of about 25 - 45 Å and in addition with carbon K_α radiation[24]. The two replicas which are reproduced in Fig. 5 in fact, show differences which are tentatively explained in terms of element distribution within the heart of chick embryo cells being picked up due to the wavelength dependence of the atomic absorption cross sections. Further details are discussed by McGowan et al.[23]. The high resolution capabilities of soft x-ray contact microscopy are demonstrated with Fig. 6 which shows a replica obtained from a thin plastic embedded section of frog retinal pigment epithelium upon exposure with wide band pass synchrotron radiation.[12] A moderate resolution SEM has been used to obtain the structures of Fig. 6a. In contrast a high resolution low-loss SEM[25] micrograph (Fig. 6b), taken from the same resist replica, shows details in the order of 100 Å even on a single melanin granule, that were completely obliterated in Fig. 6a. Apparently a resolution of about 100 Å has been obtained.

What is the ultimate resolution attainable with contact microscopy? We want to analyse this question somewhat more generally than is required for microscopy since very similar arguments also hold for lithography which is briefly discussed in the last section.

Resolution and contrast

Several factors determine the resolution of which some are wavelength dependent whereas others are not. The importance of a high resolution SEM for the resist inspection has already been pointed out (Fig. 6). At present the resolution of the SEM seems to be limited somewhat near to 20 Å. Another wavelength independent effect is due to the grain-size of the metallization. For standard coating materials e.g. Au, Pd or Au-Pd alloys, it lies between 30 and 50 Å.[26] In fact, there is a certain probability that the smallest structures with dimensions ∿50 Å to be seen in Fig. 6b might be due to grains.[12] There are two possible geometrical effects giving rise to a distortion of the shadowgraph of an object.[14] The first is penumbral blurring (δp) due to the finite size of the x-ray source (s). This effect is negligible small ($\delta p < 10$ Å) if synchrotron radiation is used, as seen from the relation $\delta p = s \cdot t/D$, where t is the distance object-wafer and T is the distance source-object. The second effect is due to non-normal incidence of the x-rays onto the sample. However, it has only to be considered for lithography application, where it can be made sufficiently small.[13-15]

More important than the above effects are the wavelength dependent effects and the behavior of the resist material which shall now be discussed. The two effects which in all practical cases determine the attainable resolution, are diffraction of the soft x-rays and the range of the hot photoelectrons that are promoted in elementary absorption events. Figure 8 shows one micrometer wide structures of bubble memory devices which have been obtained with x-ray lithography using undispersed synchrotron radiation.[15] The distance t between the wafer and the object which is here called: "mask", purpusely was chosen to be 0.5 mm and 1 mm in Fig. 8b and 8c, respectively, in order to enhance diffraction effects. Clearly, these diffraction effects are visible in Figs. 8b and 8c. With intimate contact between sample and resist, diffraction takes place only in the thickness of the sample itself and the thickness of the photoresist film. In order to in-

vestigate the resolution limitation of this case one would have to solve an extremely complicated diffraction problem. For simplicity we consider the case of an opaque edge intersecting a soft x-ray beam which at best holds for the edge of a specimen. Fresnel diffraction theory[27] gives for the distance of the first local intensity maximum $x_m=(t\cdot\lambda)^{1/2}$ with t being the distance between the object (specimen or mask) and wafer. In Fig. 9 we have plotted 0.5 x_m for various distances t as a function of wavelength. The factor 0.5 is taken to approximately include the dissolution characteristic of the PMMA resist. Figure 9 shows that intimate contact between a thin specimen and the resist is needed for very high resolution work. On the other hand, for a lot of specimens it would be useful to have a protective thin plastic film between the specimens and the resist which could be removed before the development procedure.

Hot electrons in matter have a certain penetration range until they have lost their initial kinetic energy. This range increases strongly with electron energy.[28-30] Since the resist is "exposed" by bond breaking processes of hot electrons being created in the primary photoabsorption events or in subsequent Auger processes, the range of those electrons determines the ultimate resolution attainable with a polymer resist such as PMMA.[28,29] Figure 8 also shows the range of hot electrons in PMMA as a function of the wavelength of the exciting x-rays. In addition to the calculated curve[31] three experimental data points[16] are included which have been connected by the dashed line. Considering wavelength independent effects, diffraction effects and the range of electrons, Fig. 8 tells us that the wavelength range for best resolution of about 50 Å is likely around $\lambda \sim 20$ to 40 Å.

Fortunately, the spectral sensitivity of PMMA is also very high in this wavelength range. This can be seen from Fig. 9, where the absorbed power (in $\frac{\text{Watt}}{\text{cm Å}}$) is plotted as a function of wavelength according to

$$W(\lambda) = I_o(\lambda) \cdot \alpha_{PMMA} \exp(-\alpha d)$$

$I_o(\lambda)$ is the incident flux (in Watt/cm^2 Å, including the spectral power distribution of the synchrotron radiation of DESY operating at 3.5 GeV), α_{PMMA} is the linear absorption coefficient of PMMA and α and d are the linear absorption coefficient and the thickness of either PMMA or any other filter material intersecting the radiation. Curve a of Fig. 9 corresponds to the power density at the top of the resist, whereas curve b(c) corresponds to the power density in a depth of 0.5 µm (1.0 µm) of PMMA. Thus the integral between curves a and b gives the total absorbed power density per time intervall in a 0.5 µm thick layer of PMMA. The power density behind various filters is given by curves d to g. Figure 10 shows how the total exposure P (i.e. the power density absorbed in the whole wavelength range times the exposure time) is related to the dissolution rate R of PMMA resist in different developer solutions of MIBK (methylisobutylketone) and IPA (isopropanole). With increasing exposure the dissolution rate increases nonlinearly. We obtain a rate of about 10 000 Å/min at an exposure of 5000 J/cm^3 in a (3:1) developer solution.[15] This has to be compared to the rate of about 130 Å/min of an unexposed resist. The very high contrast factor $\gamma \sim 3.5$ which corresponds to the slope of the steepest curve makes PMMA the excellent topographical recording medium in contact microscopy as well as in lithography. If we assume, for example, that a metallized replica in PMMA resist can be inspected with a SEM with a spatial resolution of 50 Å, then a contrast $\gamma \sim 3.5$ of PMMA would allow the detection of details in a specimen which produce a differental optical contrast $I+\Delta I/I \approx 1.007$. For comparison, in optical inspection the human eye can identify brightness contrasts of about 1.03. Details in the specimen of about 50 Å would require at least 1.4 μ^{-1} difference in linear absorption coefficient in order to be detected in contact microscopy. For various elemental compositions this does not seem to be unlikely (see Fig. 1 and Fig. 6b). However, it is possible that the contrast γ of PMMA is actually higher than 3.5, since in Fig. 10 only a

small number of data points has been used to construct the graphs. A peculiarity of PMMA resist is evident also from Fig. 10. At exposures above $5 \cdot 10^4$ J/cm^3 the resist starts to become less soluble than at lower exposures. At 10^5 J/cm^3 it behaves like a negative resist, whereas PMMA normally is a positive resist, i.e. exposed parts are more soluble than unexposed parts.

At this point the work of Kulipanov, Skrinsky and collaborators[32] should also be mentioned who used chalcogenid glasses as soft x-ray detectors in a contact microscopy set up. In first experiments on metallic grid structures details of about 1 µm have been obtained.

Soft x-ray lithography

Lithography with visible light is the dominant technique (proximity-projection printing) to transfer all detailed structure of masks onto semiconducting substrate materials.[33] This is one important step in electronic device fabrication such as integrated circuits. At present, commercial microcircuits have smallest structures of about 2.5 µm. However, there are several reasons for increasing the degree of miniaturization; for example, speed of operation, power consumption, circuit reliability and cost per electric function. With computer controlled scanning electron beam systems [34] complex pattern can be generated with dimensions of about 500 Å, limited due to the inherent problem of electron scattering in e-beam resists.[28,29] Such small dimensions are far beyond present and near future technical needs, but one expects a need for a micron and perhaps submicron structures around 1985.[35] Mass production costs with scanning e-beam systems are one to two orders of magnitude higher than with photolithography techniques. But unfortunately diffraction effects do not allow a fabrication of submicron structures with proximity photolithography with visible light. Various efforts habe been made to produce submicron line width pattern, e.g., by using ultraviolet light[36] or by using special conformable masks with intimate contact to the wafer.[33]

However, the most promising results have been obtained with x-ray lithography.[13-15,33]

The principle of x-ray lithography (see Fig. 11) is the same as that of contact microscopy or microradiography.[1] An object is kept close, but not in contact, to a thin resist film on a metallized silicon substrate. The object is the mask containing complex structures necessary to produce electronic circuits. The first mask, and that is important to note, is fabricated by the scanning electron beam system. The device pattern is made in highly absorbing material (e.g. Au, Re) supported by a highly transmitting substrate material (e.g. Be, Si_3N_4, mylar, Al_2O_3). The mask-wafer combination is exposed to x-rays and subsequently developed in the same manner as described above. The remaining resist serves as a protective coating for subsequent processing steps which include dry ion or wet chemical etching, electroplating, doping etc. For the production of large scale integrated circuits several exposures with different masks on the same wafer are necessary. This implies an extreme alignment accuracy, if submicron or even micron lines are to be matched. Certainly this is one of the most severe problems in the fabrication process. But simple devices have already been produced by x-ray lithography.[13,33,37] Some of the circuits of magnetic bubble devices[37] can be fabricated with a single mask. Figure 7, for example, shows basis structures in PMMA resist for such a device. As mentioned above, the exposure has been made with synchrotron radiation of the DESY synchrotron. Figure 12 displays a SEM micrograph of the metal structure of a bubble memory device. The metal pattern shown are 1 µm wide and about 3 µm high. It is one of the advantages of x-ray lithography that even higher aspects ratios (height : width of structures) can easily be obtained, if soft x-ray radiation is used.[4,6,33,39]

Based on our discussion in the previous paragraphs, we can summarize the advantages of soft x-ray lithography with synchrotron radiation for an eventual fabrication of circuits with structures 1 µm to 0.1 µm as follows: An optimum wave-

length range ($\lambda \gtrsim 10$ Å) can be chosen such that the contrast of a mask (e.g. Re on mylar) is sufficiently high ($K \gtrsim 10:1$) even for a relatively thin absorber film of 0.3 µm Re (compare Fig. 1). A contrast of 3:1 is often considered to be sufficient.[6,14,33] The diffraction limited resolution depends on mask-wafer distance. Figures 7 and 8 suggest that at least 100 µm are allowed for micron or even submicron line width. Proximity effects due to electron scattering range are negligible small as well as geometrical distortion and penumbra (Fig. 8). Storage rings with energies above 700 MeV and high circulating currents appear to allow exposure times of less than a minute, even, if additional filters are used (seperating e.g. exposure vessel, backfilled with He exchange gas, from a high vacuum beam line to the storage ring). A further advantage is the apparent insensitivity of x-ray lithography to dust and contamination,[6] since most of the dust particles consist of organic material having a weak absorption.

Of course, soft x-ray lithography with synchrotron radiation also has disadvantages. Suitable storage rings are not readily available and construction and maintenance costs are very high. But strong efforts are being made to build new facilities.[40] For several applications the collimation of synchrotron radiation which is a function of wavelength might cause problems, as well as the ultrahigh vacuum in a storage ring. The radiation damage to the substrate of an x-ray mask and wafer heating at power density levels 0.1 to 1 Watt/cm^2 are not well known. There are further points, but none of them seem to be fundamental in nature.

Conclusions

On the whole x-ray lithography appears to be a very promising exposer technique in micron and submicron device fabrication. But it is important to keep in mind that with high resolution mask replication also high resolution processing steps, including mask-wafer alignment and appropriate circuit design, are required. At the present time those steps seem to set the limitation for the attainable size

of structures. With contact microscopy of biological specimens a resolution of about 100 Å has been obtained. Future efforts in microscopy are directed towards an investigation of biological specimens in vitro with monochromatized synchrotron radiation in order to enhance the contrast for specific kinds of atoms in certain regions of the sample.

Acknowlegement

The author has benefited from many discussions with E. Spiller and J.Wn. McGowan with whom the described contact microsocpy experiments have been carried out.

References

1. P. Goby, C.R.Acad.Sci. Paris 156, 686 (1913)
2. P. Kirkpatrik and H.H. Patte, Jr., Handb. Phys. Bd. 30, Springer Verlag Berlin, Heidelberg, New York (1957)
3. V.E. Cosslett and W.E. Nixon, X-ray microscopy, University Press, Cambridge (1960)
4. E. Spiller, R. Feder, J. Topalian, D. Eastman, W. Gudat and D. Sayre, Science 191, 1172 (1976)
5. P. Horowitz and J.A. Howell, Science 178, 608 (1972)
6. E. Spiller and R. Feder, X-ray Lithography in Topics in Appl. Phys. Vol. 22, ed. H.J. Queisser, Springer Verlag Berlin, Heidelberg, New York (1977)
7. R.P. Haelbich and C. Kunz, private communication
8. B. Niemann, D. Rudolph and G. Schmahl, Appl.Opt. 15, 1882 (1976)
9. G. Schmahl, Proc. Vth Int.Conf. on VUV Rad.Phys., Montpellier, Sept. 5.-9. (1977)
10. S. Aoki, Y. Ichihara and S. Kikuta, Japan.J.Appl.Phys. 11, 1857 (1972)
11. A.M. Kondratenko and A.N. Skrinski, preprint No. 76-105, Institut of Nuclear Physics, Novosibirsk (1976)
12. R. Feder, E. Spiller, J. Topalian, A.N. Broers, W. Gudat, B.J. Panessa, Z.A. Zadunaisky and J. Sedat, Science 197, 259 (1977)
13. D.L. Spears and H.J. Smith, Electron.Lett. 8, 102 (1972)
14. D.L. Spears and H.I. Smith, Solid State Technol. 15, 21 (1972)
15. E. Spiller, D.E. Eastman, R. Feder, W. Grobman, W. Gudat and J. Topalian, J. Appl.Phys. 47, 5450 (1976)
16. R. Feder, E. Spiller and J. Topalian, J.Vac.Sci.Technol. 12, 1332 (1975)
17. R. Haensel, K. Radler, B. Sonntag and C. Kunz, Sol.State Commun. 7, 1495 (1969)
18. D. Sayre, J. Kirz, R. Feder, D.M. Kim and E. Spiller, Science 196, 1339 (1977)
19. H. Wolter, Ann. der Physik 6, 94 and 286 (1952)
20. E. Spiller, Appl.Optics, 15, 2333 (1976)
21. R.P. Haelbich and C. Kunz, Opt.Commun 17, 187 (1976)

22. S. Aoki and S. Kikuta, Japan J.Appl.Phys. 13, 1385 (1974)
23. J.Wn. McGowan, B. Borwein, J.A. Medeiros, T. Beveridge, J.D. Brown, E. Spiller, R. Feder, J. Topalian and W. Gudat, submitted for publication
24. The exposure with carbon K_α-radiation were made at the IBM T.J. Watson Research Center
25. O.C. Wells, A.N. Broers and C. Bremer, Appl.Phys.Lett. 23, 353 (1973)
26. S.V. Chatterjee, Naturw. 45, 106 (1958)
27. see e.g. A. Sommerfeld, Optik, Akademische Verlagsgesellschaft, Leizig 1964 M. Born and E. Wolf, Principles of Optics, London, Oxford (1964)
28. D.F. Kyser and N.S. Viswanathan, J.Vac.Sci.Technol. 12, 1305 (1975)
29. M. Hatzakis, Appl.Phys.Lett. 18, 7 (1971)
30. Ch. Feldmann, Phys.Rev. 117, 455 (1960)
31. The range of hot electrons has been calculated on the basis of an empirical formula given in Ref. 30
32. G.N. Kulipanov, A.N. Skrinski et al., Preprint No. 77-10, Institute of Nuclear Physics, Novosibirsk (1977)
33. H. Smith, Proc. IEEE, 62, 1361 (1974)
34. see e.g. a) Proc. 7th Int.Conf. Electr.Ion.Beam Sci.Technol. ed. R. Bakish, Princeton (1976)
    b) Proc. 13th Sym.Electr.Ion Phot.Beam Technol., ed.R.F.W. Pease, J.G. Skinner, J.Vac.Sci.Technol. 12, No 6 (1975)
    c) Proc.Int.Conf. on Microlithography, Paris, 21.-24. June (1977)
35. A.C. Tobey, in Ref. 34c)
36. B.J. Lin, page 1317 of Ref. 34b)
37. E. Spiller, R. Feder, J. Topalian, E. Castellani, L. Romankiw and M. Heritage, Sol.State Technol. 19, 62 (1976)
38. E. Spiller, R. Feder, J. Topalian, Symposium of Synchrotron Radiation, Denver, Febr. 20.-25. (1977)
39. B. Fay, J. Trotel, Y. Petroff, R. Pinchaux and P. Thiry, Appl.Phys.Lett. 29 370 (1976)
40. A.L. Robinson, Science 197, 148 and 448 (1977)

Figure Captions

Fig. 1 Linear absorption coefficient of some of the most absorbing and most transparent materials for soft x-rays.[16,17] PMMA (polymethylmethacrylate) is a positive x-ray resist. The absorption coefficient of the compounds is obtained from the elemental mass absorption coefficients.[16]

Fig. 2 Layout of a scanning x-ray microscope using synchrotron radiation (from Horowitz and Howell[5])

Fig. 3 Principle of contact microscopy: I The incident x-ray flux is modified by the absorption profile of the specimen and absorbed in the x-ray resist. II After removal of the specimen a resist replica of the specimen's optical density is obtained in a wet development procedure. This can be viewed with a scanning electron microscope after metallization.

Fig. 4 Replication of diatoms with soft x-ray synchrotron radiation, effective wavelength range 25 Å to 44 Å, exposure time 10 min in a distance of 40 m from the source point and no focussing of the radiation, effective exposure about 1200 J/cm^3. (from Spiller et al.[4])

Fig. 5 Heart of chick embryo cells replicated with synchrotron radiation and with Carbon K_α radiation. Nucleus (N), nucleolus (NO), microspikes (MS) and microtubules (MT) are identified. C denotes cell fragments due to incomplete removal of the specimens. The prominence of the nucleus in the lower replica is tentatively ascribed to build up of phosphorus (from McGowan et al.[23])

Fig. 6 Synchrotron radiation ($\lambda \sim 25$ to 44 Å) replica obtained from thin (~ 700 Å) plastic embedded section of frog retinal pigment epithelium. Figure 6a shows blurred structures of elliptical protuberances which are representative of melanin granules, obtained with a commercial SEM. Figure 6b shows detailed structures of a melanin granule as small as 100 Å or less, obtained with a high resolution SEM. (from Feder et al.[12])

Fig. 7 Synchrotron radiation replication of 1 µm linewidth structures in 0.7 µm (a) and (c) and 0.5 µm (b) thick gold masks on 6 µm mylar. For 0.5 mm (b) and 1 mm (c) mask-wafer spacings diffraction fringes are obtained. Effective wavelength range $\sim$3 Å to 15 Å. (from Spiller et al.[15]

Fig. 8 The effective range of fast photo- and Auger electrons which are generated in PMMA resist by absorbed x-ray photons, is plotted versus the wavelength of the x-rays. The resolution limitation due to Fresnel diffraction is also plotted versus wavelength for different distances t between object (mask) and resist material. Electron range and diffraction effects determine the optimum resolution of about 50 Å for contact microscopy somewhere between $\lambda \sim 20$ and 40 Å, since wavelength independent effects are smaller.

Fig. 9 Power absorbed in PMMA resist as a function of wavelength for synchrotron radiation from DESY in a distance of 40 m from the source point. Curve (a) gives the power density per Å at the top of the resist, (b) in a depth of 0.5 µm and (d) in a depth of 1 µ PMMA. Curves (c) and (e)-(g) correspond to (a) plus various filters in the beam: (c) 1.5 µm of parylene N; (e) 12 µm of beryllium; (f) 6 µ mylar and (g) 6 µ of mylar + 0.8 µ of gold. (from Spiller et al.[15])

Fig. 10 Dissolution rare versus exposure for resist PMMA. Developer is methylisobutylketone (MIBK) diluted with isopropanole (IPA). At a heavy exposure of 5000 J/cm^3 the contrast factor γ (the slope of the graphs) is at least 3.5, since points with an arrow represent a lower limit to the dissolution rate. (from Spiller et al.[15]).

Fig. 11 Illustration of the x-ray lithography technique and subsequent fabrication steps.

Fig. 12 Bubble memory devices can be fabricated with s single mask which is produced in a scanning electron beam system. The metal pattern shown are 1 micrometer wide and about three times as high. It is one of the advantages of x-ray lithography that high aspect ratios are attainable. (from Spiller et al.[38]).

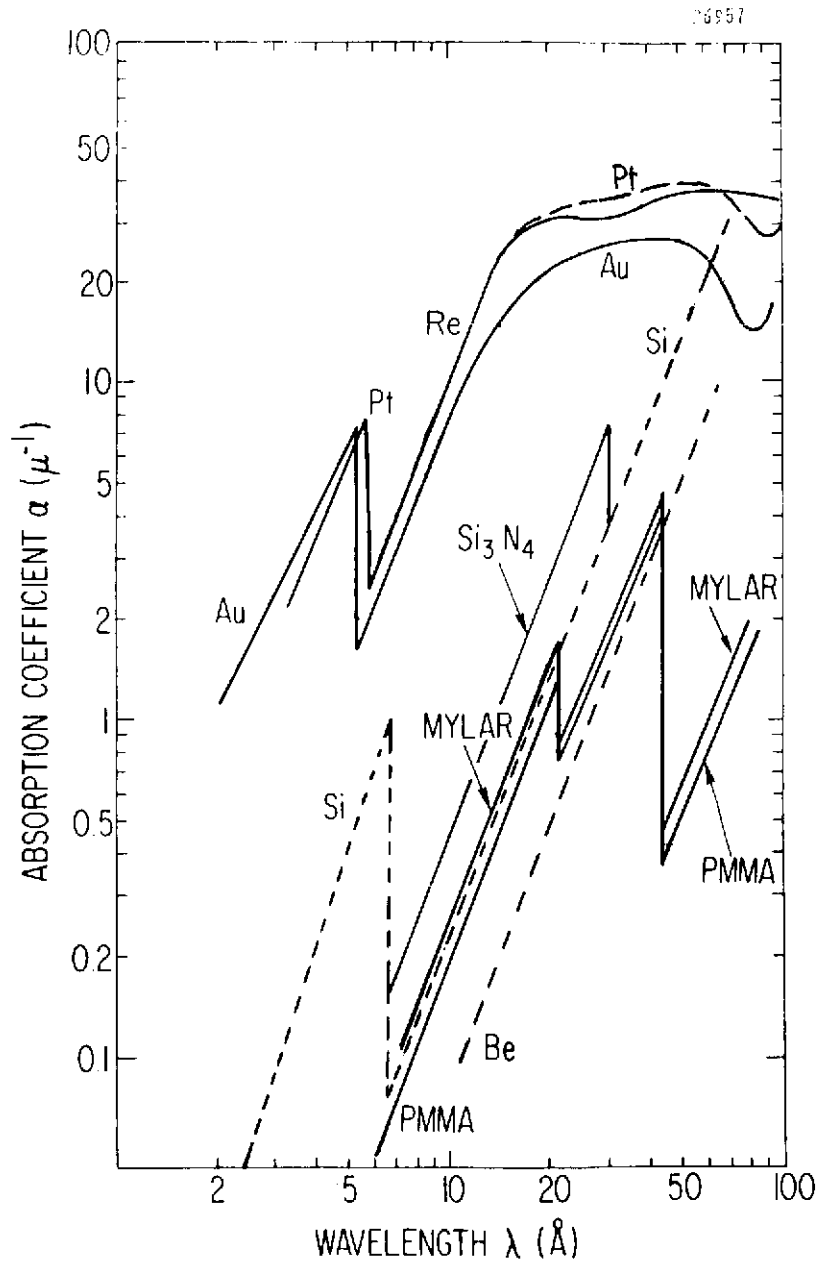

Fig. 1

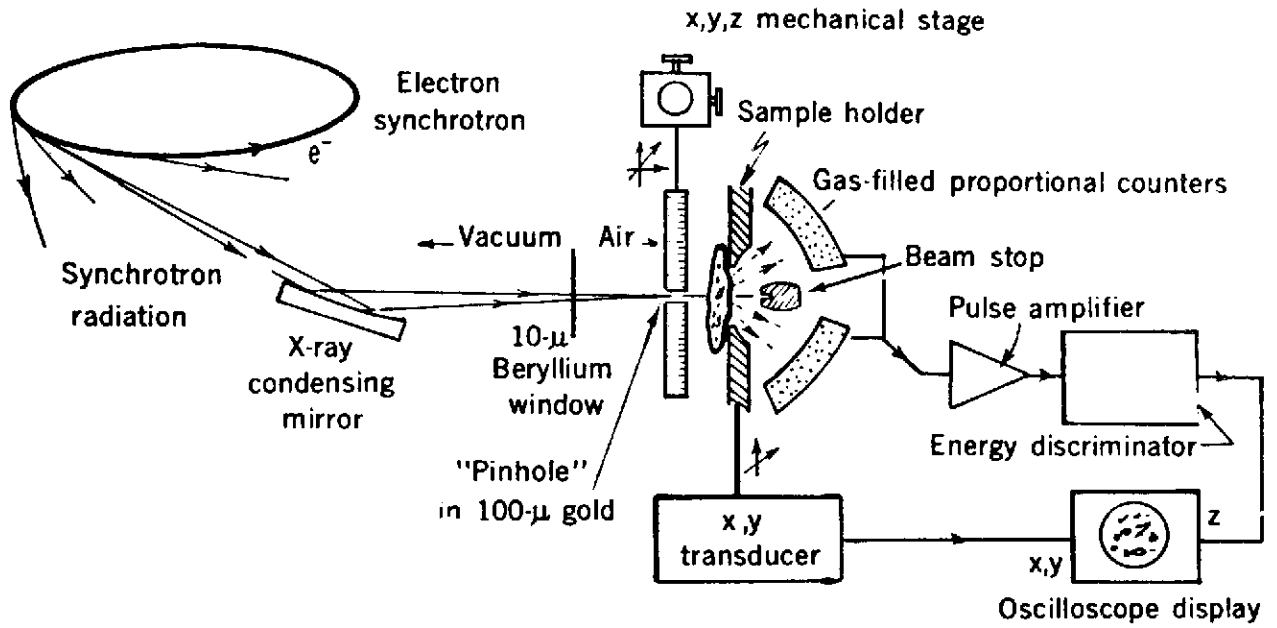
x,y,z mechanical stage
Electron synchrotron
e⁻
Sample holder
Gas-filled proportional counters
Vacuum
Air
Beam stop
Synchrotron radiation
Pulse amplifier
X-ray condensing mirror
10-μ Beryllium window
Energy discriminator
"Pinhole" in 100-μ gold
x,y transducer
z
x,y
Oscilloscope display

Fig. 2

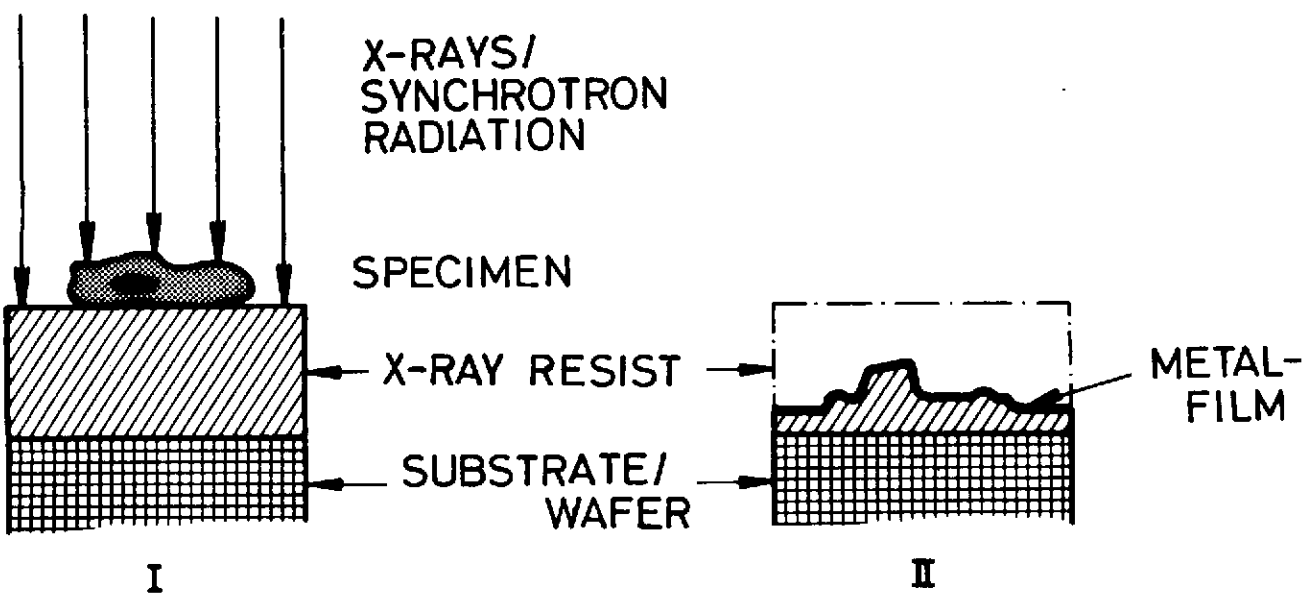
X-RAYS/ SYNCHROTRON RADIATION
SPECIMEN
X-RAY RESIST
SUBSTRATE/ WAFER
METAL-FILM
I
II

Fig. 3

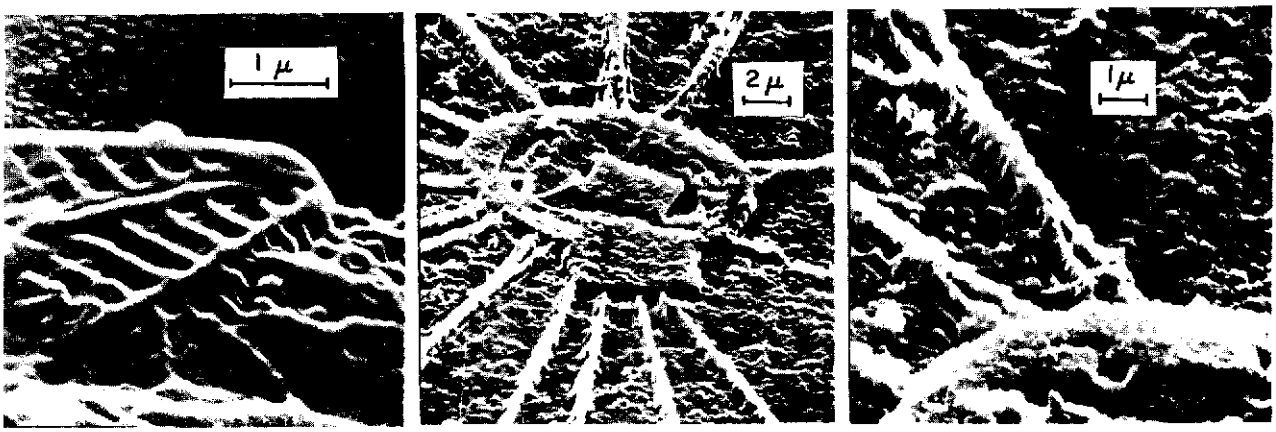
1 μ
2 μ
1 μ
a
b
c

Fig. 4

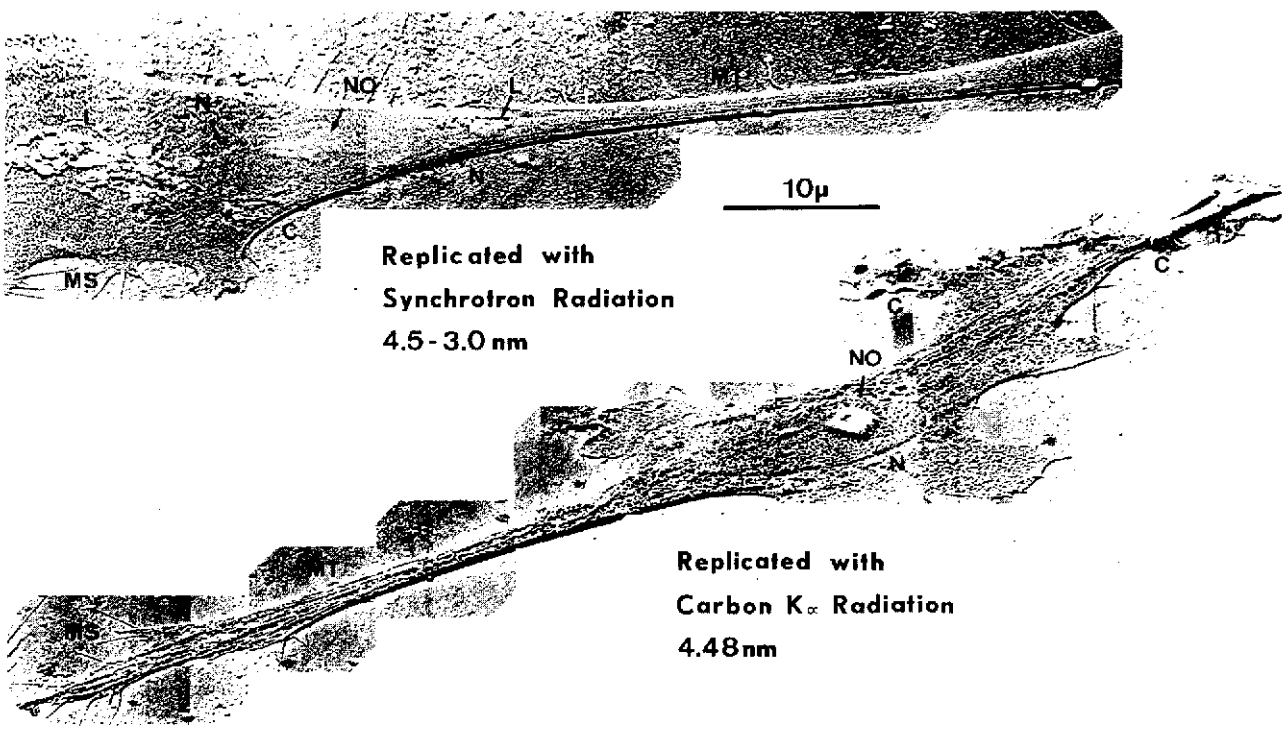
NO
MT
N
C
MS
10μ
Replicated with
Synchrotron Radiation
4.5 - 3.0 nm
C
NO
N
MT
MS
Replicated with
Carbon Kα Radiation
4.48nm

Fig. 5

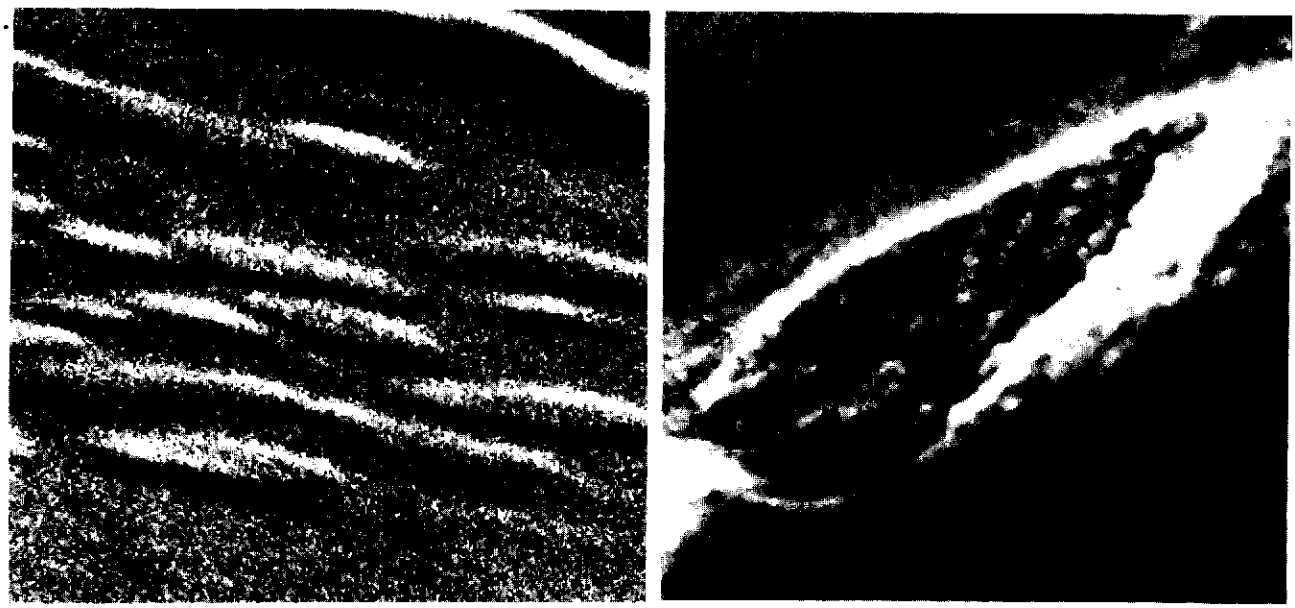

Fig. 6

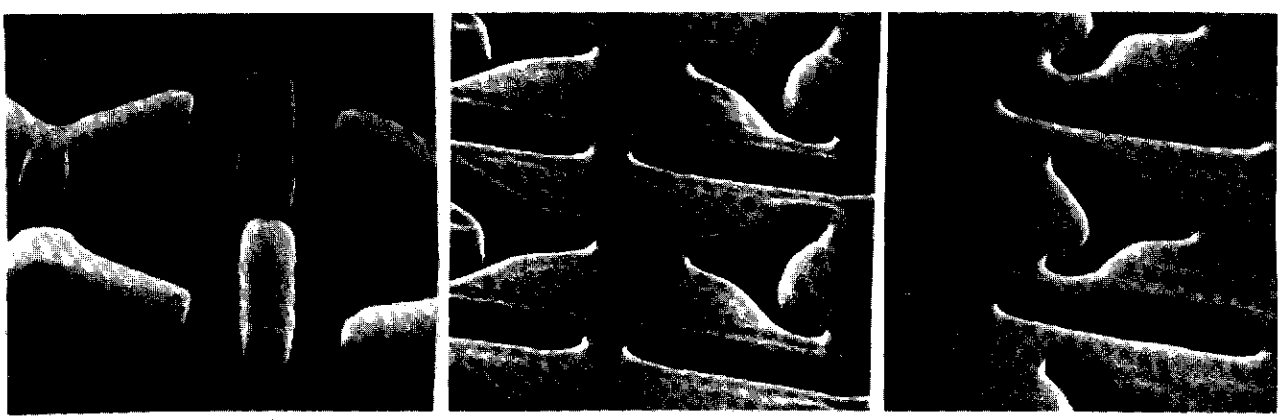

Fig. 7

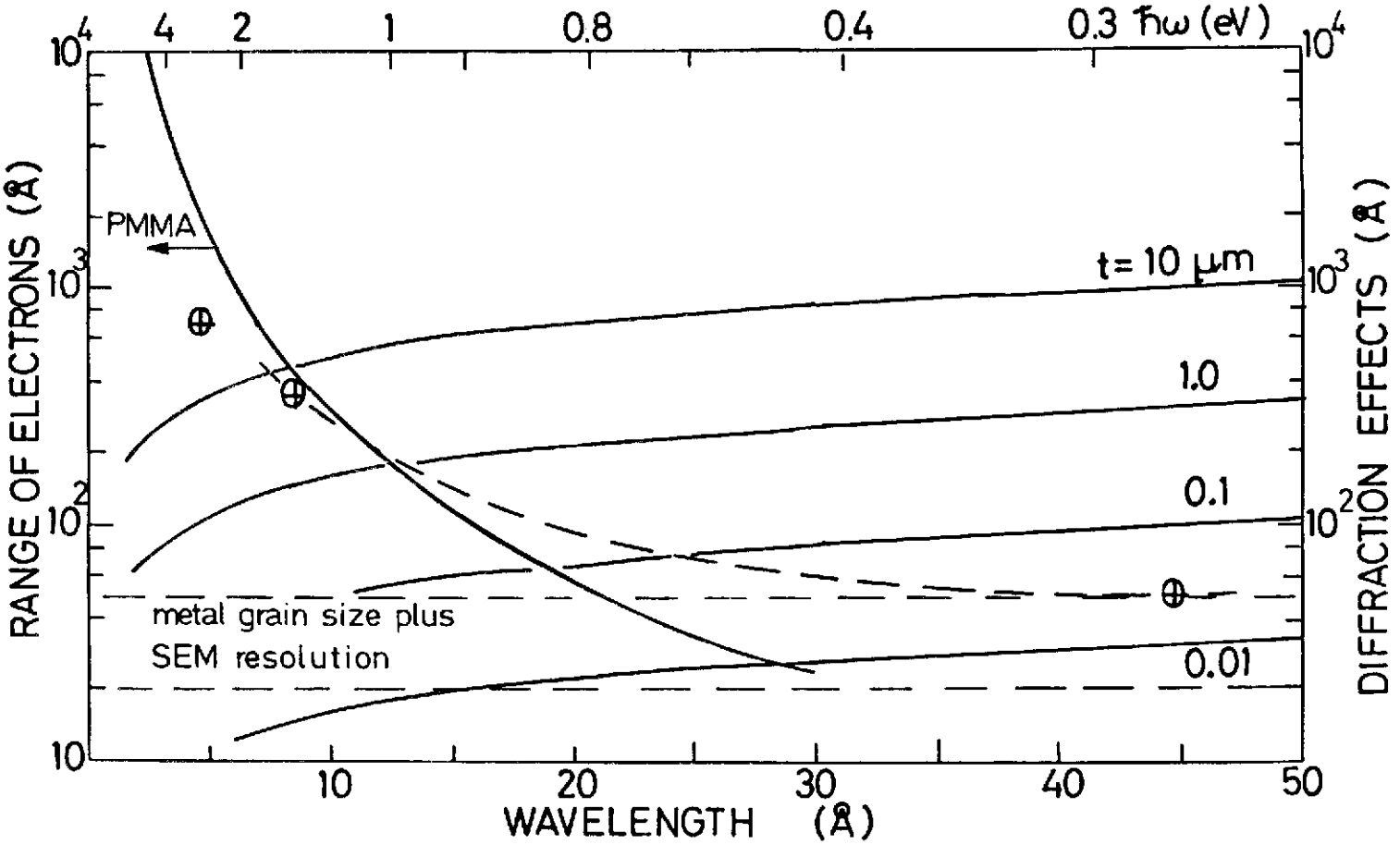
4
2
1
0.8
0.4
0.3 ħω (eV)
RANGE OF ELECTRONS (Å)
DIFFRACTION EFFECTS (Å)
PMMA
t= 10 μm
1.0
0.1
0.01
metal grain size plus
SEM resolution
WAVELENGTH (Å)

Fig. 8

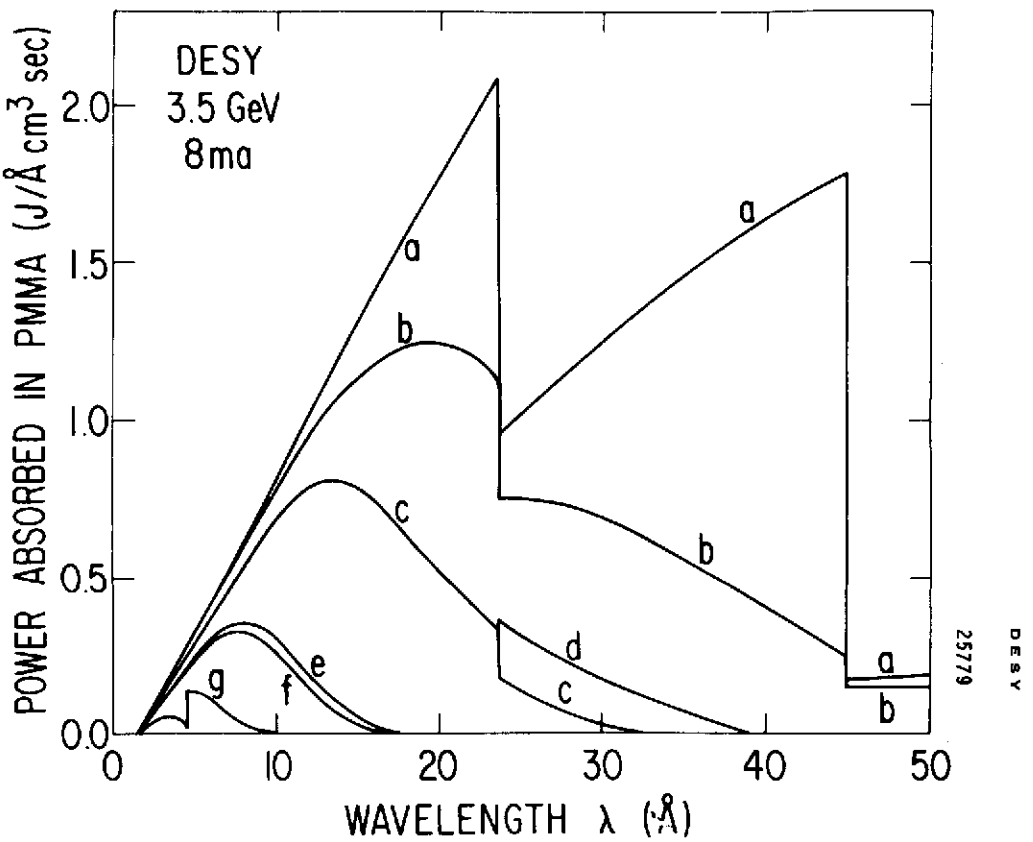
DESY
3.5 GeV
8ma
POWER ABSORBED IN PMMA (J/Å cm³ sec)
WAVELENGTH λ (Å)
a
b
c
d
e
f
g
DESY
25779

Fig. 9

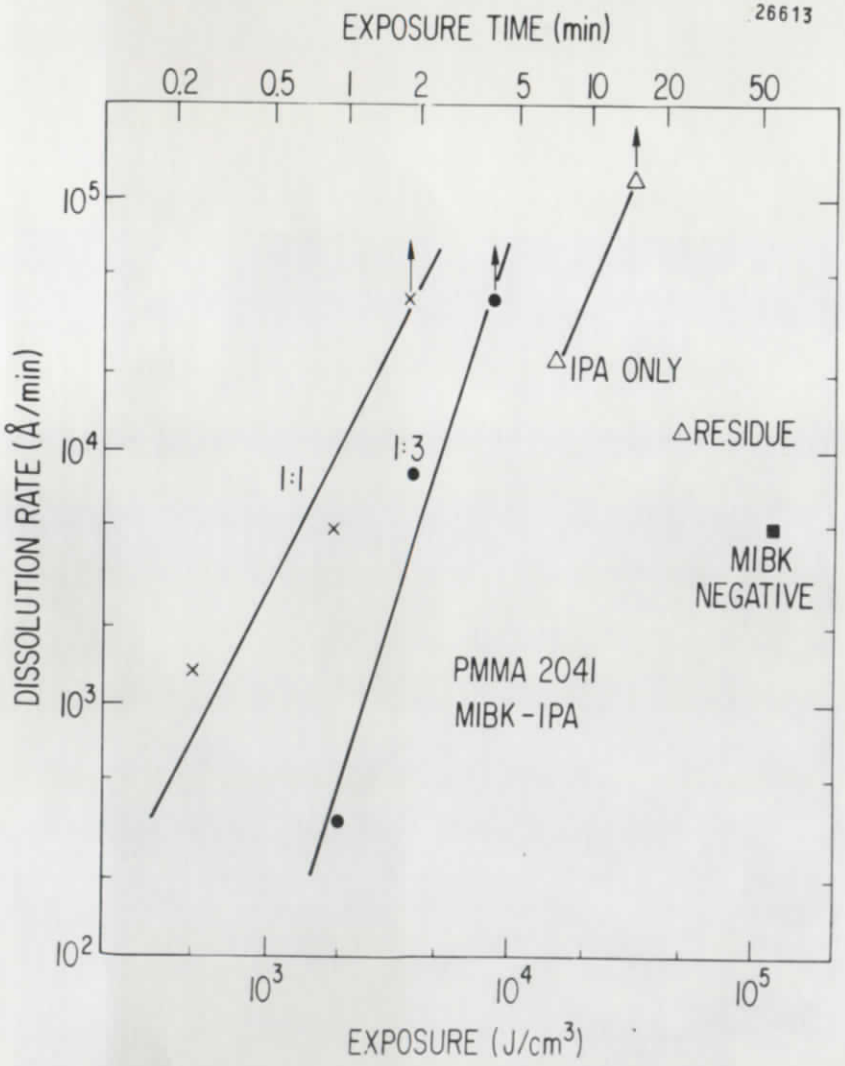
EXPOSURE TIME (min)
0.2
0.5
1
2
5
10
20
50
DISSOLUTION RATE (Å/min)
10^5
10^4
10^3
10^2
1:1
1:3
△IPA ONLY
△RESIDUE
■ MIBK NEGATIVE
PMMA 2041
MIBK-IPA
10^3
10^4
10^5
EXPOSURE (J/cm^3)

Fig. 10

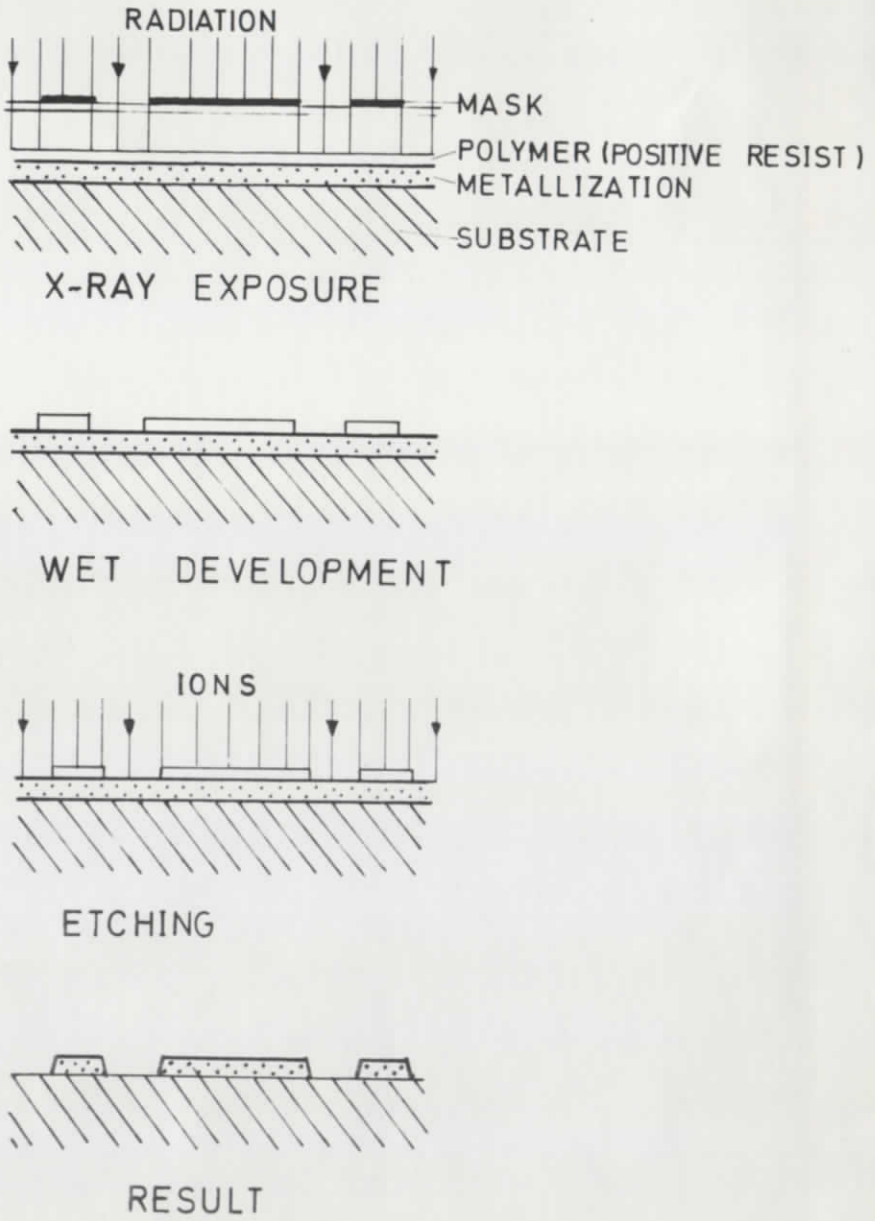
RADIATION
MASK
POLYMER (POSITIVE RESIST)
METALLIZATION
SUBSTRATE
X-RAY EXPOSURE
WET DEVELOPMENT
IONS
ETCHING
RESULT

Fig. 11

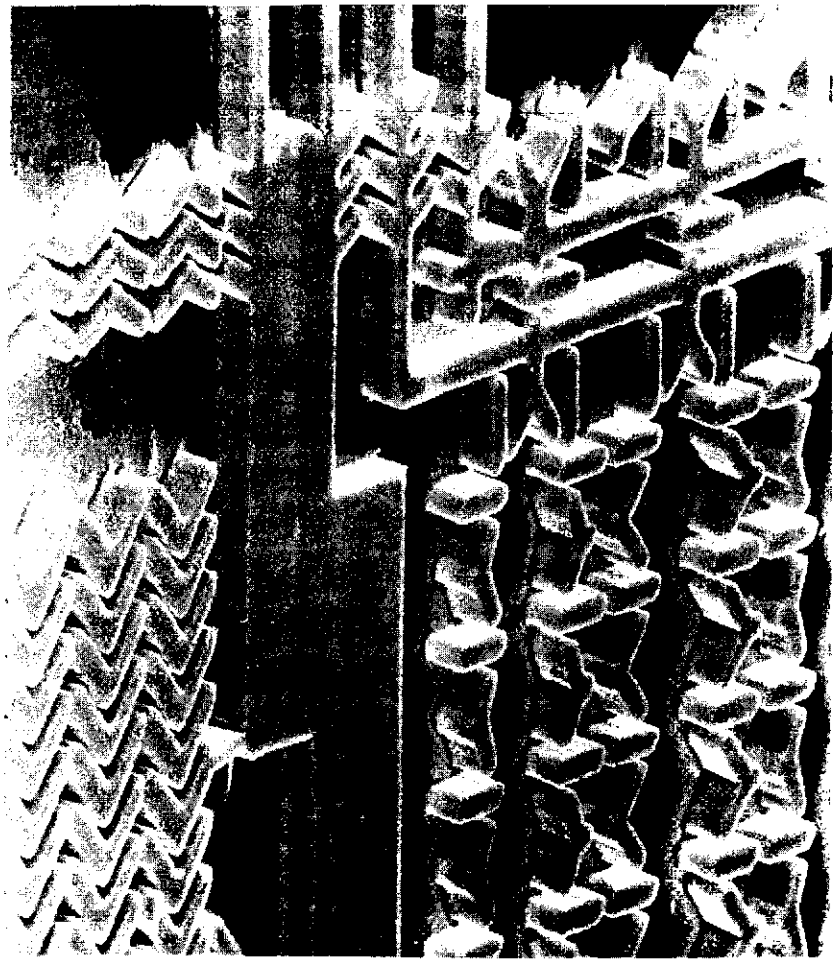

Fig. 12